

Giant Dielectric Anomaly of a Metal–Organic Perovskite with Four-Membered Ring Ammonium Cations**

Biao Zhou, Yuji Imai, Akiko Kobayashi,* Zhe-Ming Wang, and Hayao Kobayashi*

Ferroelectric materials with dielectric constants larger than 10^4 over a broad temperature range near room temperature have great potential for technological applications. Such highly polarizable materials have been found only in the perovskite-related metal oxides called relaxors.^[1–3] Recently, the development of molecule-based highly polarizable materials has attracted increasing interest. For example, antiferroelectric and ferroelectric porous coordination polymer crystals with guest water molecules, a ferroelectric crystal consisting of single-component molecules with very large spontaneous polarization, and an exotic ferroelectric crystal based on ‘supramolecular rotators’ have been reported.^[4,5] However, there has been no report of molecule-based solids with broad dielectric peaks higher than 10^4 .

High polarizability in a material is usually related to its structural freedom, such as the orientational motion of the permanent electric dipole and the freezing of the optical lattice vibration. Since molecules generally possess large structural freedom, the realization of molecule-based materials exhibiting giant polarizability will be a promising challenge. One of the structural freedom characteristics of the molecules is the ring-puckering motion of four-membered-ring molecules. It has been known for over half a century that the four-membered-ring molecules, such as trimethylene sulfide, trimethylene oxide, and cyclobutane as well as five-membered-ring molecules with one double bond, such as 2,5-dihydrofuran, have double minimum potentials for the out-of-plane bending deformation of the molecule and therefore exhibit characteristic ring-puckering molecular vibrations (Figure 1a).^[6–8] If the energy barrier between the double minima is sufficiently high, the molecule will adopt a non-

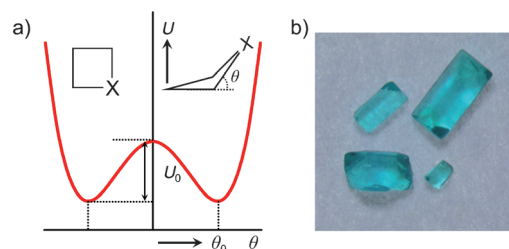


Figure 1. a) A schematic drawing of double-minimum potential $U(\theta)$ for out-of-plane-bending deformation of four-membered-ring molecules. The observed values of θ_0 and U_0 are 29° , 515 cm^{-1} for $X=\text{CH}_2$ (cyclobutane); 28° , 274 cm^{-1} for $X=\text{S}$ (trimethylene sulfide); 0° , 15 cm^{-1} for $X=\text{O}$ (trimethylene oxide).^[13] For $X=\text{NH}$ (azetidine), the double-minimum potential becomes asymmetric ($U_0 \approx 440\text{ cm}^{-1}$).^[13] b) Crystals of $[(\text{CH}_2)_3\text{NH}_2][\text{Cu}(\text{HCOO})_3]$.

planar structure even at high temperatures. However, if the magnitude of the energy barrier is thermally accessible, it may be possible that the molecule adopts a nonplanar structure at low temperatures and a planar structure at high temperatures. In such a case, it would be possible for the crystal to exhibit a large dielectric susceptibility coupled with a cooperative change of the molecular conformation. However, to our knowledge, studies to develop molecule-based dielectrics utilizing the conformational freedom characteristics of the four-membered-ring molecule have not been reported. Herein we report a metal–organic perovskite containing four-membered-ring ammonium cations, $[(\text{CH}_2)_3\text{NH}_2][\text{Cu}(\text{HCOO})_3]$, which exhibits a very broad and unprecedentedly large dielectric peak near 280 K.

We have reported the magnetic properties of the metal formate crystal with cyclotrimethyleneammonium cations (or azetidinium cation, $(\text{CH}_2)_3\text{NH}_2^+$), $[(\text{CH}_2)_3\text{NH}_2][\text{Mn}(\text{HCOO})_3]$,^[9] which has been regarded as a metal–organic perovskite ABX_3 (A = ammonium cation, $B = \text{M}^{2+}$ ($\text{M} = \text{Zn}$, Mn), and $X = \text{HCOO}^-$) with three-dimensional CaTiO_3 -like structure.^[10–12] Similar to well-known inorganic ferroelectric and antiferroelectric perovskites such as BaTiO_3 and PbZrO_3 , these metal–organic perovskites have been reported to exhibit dielectric transitions.^[10,11]

With the aim of utilizing the ring-puckering molecular motion in inducing the dielectric transition of metal–organic perovskite, we have prepared the analogous $[(\text{CH}_2)_3\text{NH}_2][\text{Cu}(\text{HCOO})_3]$. The crystals were obtained by the solution diffusion method according to the reported procedure (Figure 1b).^[9] The crystal structure was determined at 123, 180, 243, 260, 300, and 333 K. At room temperature, $[(\text{CH}_2)_3\text{NH}_2][\text{Cu}(\text{HCOO})_3]$ is isostructural to $[(\text{CH}_2)_3\text{NH}_2][\text{Mn}(\text{HCOO})_3]$, which belongs to the orthorhombic system with the space

[*] Dr. B. Zhou, Y. Imai, Prof. A. Kobayashi, Prof. H. Kobayashi
Department of Chemistry, College of Humanities and Sciences
Nihon University, Sakurajosui, Setagaya-ku, Tokyo 156-8550 (Japan)
E-mail: akoba@chs.nihon-u.ac.jp
hayao@chs.nihon-u.ac.jp

Prof. Z.-M. Wang
College of Chemistry and Molecular Engineering, Peking University
Beijing 100871 (P. R. China)

[**] This work was financially supported by Grants-in-Aid for Scientific Research (B) (No. 20350069), Young Scientists (B) (No. 21750153), and Innovative Areas (20110003) from the Ministry of Education, Culture, Sports, Science and Technology of Japan. The study was also supported by the ‘Strategic Research Base Development’ Program for Private Universities subsidized by MEXT (2009) (S0901022). The authors thank Mr. Y. Karatsu (Fuso-Seishakusho Co.) for the construction of the instruments for dielectric measurements and useful discussions.

Supporting information for this article is available on the WWW under <http://dx.doi.org/10.1002/anie.201105111>.

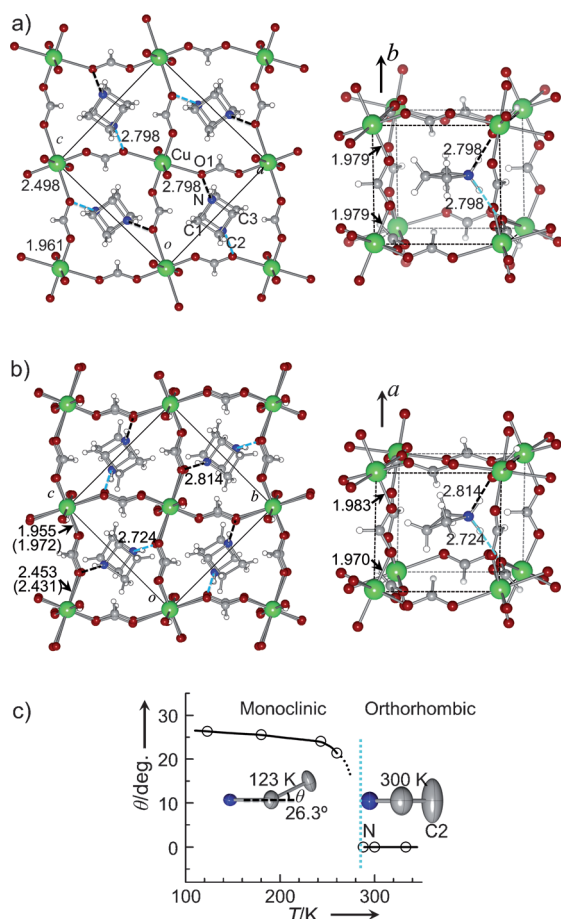


Figure 2. a) The crystal structure of $[(\text{CH}_2)_3\text{NH}_2][\text{Cu}(\text{HCOO})_3]$ at 300 K viewed along the b axis of the orthorhombic lattice and the structure of the metal formate framework containing azetidinium cations. b) The monoclinic crystal structure and the metal formate framework with azetidinium cations at 123 K. There are six crystallographically independent Cu–O bonds. The Cu–O bond lengths in parentheses are those in the neighboring bc layer below $a/2$. c) The temperature dependence of the magnitude of the ring-puckering deformation of an azetidinium cation, where $\theta = 180^\circ$ (the dihedral angle between the C1–N–C3 and the C1–C2–C3 planes; see Figure 2a). The side views of the cation at 300 and 123 K are also presented, where the thermal ellipsoids are drawn at the 30% (300 K) and 50% (123 K) probability levels.

group $Pnma$.^[9] As seen from Figure 2a, the copper atoms and the bidentate formate ligands form a metal formate framework containing azetidinium cations. The crystal structure viewed along the b axis possesses an approximately fourfold symmetry, owing to the pseudo-tetragonal lattice constants ($a \approx c$). The Cu^{2+} ions are octahedrally coordinated by the six oxygen atoms of the surrounding bridging HCOO^- ligands, where the three crystallographically independent Cu–O bond lengths (1.961(1), 1.979(1), and 2.498(1) Å at 300 K) indicate Jahn–Teller distortion of the coordination structure around Cu^{2+} . The longest Cu–O bond (2.498 Å) and the shortest Cu–O bond (1.961 Å) appear alternately along the $a + c$ (or $a - c$) direction. That is, adjacent Cu atoms in the ac plane are bridged by the longest and shortest Cu–O bonds. The azetidinium cation is on the mirror plane perpendicular to

the b axis and therefore adopts a planar structure. The nitrogen atom of the cation is bonded to the oxygen atom of the formate ligand (O1) by a hydrogen bond ($r(\text{N} \cdots \text{O}1) = 2.798$ Å at 300 K; see Figure 2a). Considering the hydrogen bond of the N atom and the freedom of the ring-puckering molecular motion of the azetidinium cation, it is natural that the N atom has a relatively small thermal factor and the C2 atom has a large anisotropic thermal factor, indicating the large out-of-plane bending molecular motion (Figure 2c). The planar structure and large thermal factor of the azetidinium cation at 300 K suggested the possibility of a structural phase transition associated with the freezing of the ring-puckering molecular deformation at a low temperature. The hydrogen bond between the N and O1 atoms and the repulsive force between the CH_2 group of the cation and the CH group of the formate anion is consistent with the deformation of the metal formate framework (shrinkage along the N–C2 direction and expansion along the C1–C3 direction; see Figure 2a). At the same time, the N–C2 direction of the four-membered-ring cation rotates from the $a + c$ (or $a - c$) direction. The metal formate frameworks elongated along the $a + c$ direction and those elongated along the $a - c$ direction are arranged alternately along the $a + c$ and $a - c$ directions (Figure 2a).

The temperature dependence of the magnetic susceptibility was measured down to 2 K. Above 30 K, the susceptibility was well-fitted by the Bonner–Fisher antiferromagnetic chain model. A spin-canted antiferromagnetic transition was observed at 5 K and a weak ferromagnetic hysteresis was observed, which are consistent with the existence of two crystallographically independent Cu ions bridged by a non-centrosymmetric formate ligand at low temperatures (Figure 2b). This magnetic behavior is similar to that of $[\text{Gua}][\text{Cu}(\text{HCOO})_3]$ ($\text{Gua} = (\text{C}(\text{NH}_2)_3)^+ = \text{guanidinium cation}$).^[14] As already pointed out,^[14] the one-dimensional nature of the Cu^{2+} spin system is consistent with the structural feature in which the neighboring Cu atoms along the a axis (of the low-temperature monoclinic structure) are bridged by O–CH–O ligands through only short Cu–O bonds (1.970 and 1.983 Å at 123 K; Figure 2b). Furthermore, the magnetic interactions along the $b + c$ and $b - c$ directions of the monoclinic lattice will become small because the neighboring Cu^{2+} ions in the ac plane are bridged through O–CH–O ligands with long (2.431 and 2.453 Å at 123 K) and short (1.972 and 1.955 Å at 123 K) Cu–O bonds (Figure 2b).

The dielectric constants ($\epsilon = \epsilon_1 - i\epsilon_2$) were measured at 85–330 K for electric fields applied parallel and perpendicular to the b axis of the orthorhombic lattice. Essentially identical results were obtained for both directions. As mentioned above, a dielectric anomaly is expected to be observed upon cooling the sample if the ring-puckering molecular deformation of the azetidinium cation is frozen at low temperature. As shown in Figure 3a, the dielectric constant was found to exhibit an anomalous dielectric peak near 270 K. At first, this dielectric peak could not be observed reproducibly, because the magnitude of the peak of ϵ_1 showed an extremely strong dependence on the cooling and heating rates. A sufficiently large peak was observed only when the speed of the temperature change was very small ($< 10^\circ \text{h}^{-1}$). When the speed of

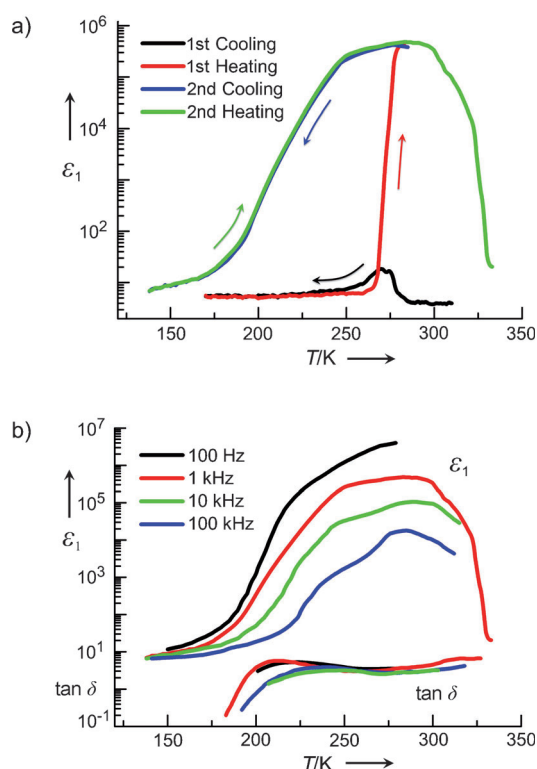


Figure 3. a) A typical example of the temperature dependences of the dielectric constants (ϵ_1) in the first cooling cycle and the subsequent heating cycle (at 1 kHz). The heating rate in the range 270–280 K was very small ($< 2^\circ \text{h}^{-1}$). The dielectric constant at low temperatures was omitted because it was very small and showed featureless temperature dependence. b) Temperature dependence of the dielectric constant (ϵ_1) at frequencies of 100 Hz to 100 kHz. To avoid the disappearance of the highly polarizable state upon heating the sample, the maximum temperature did not exceed 300 K in most of the heating cycles. The temperature dependence of the loss tangent ($\tan \delta = \epsilon_2/\epsilon_1$) is also presented.

the temperature change was not small ($> 2^\circ \text{min}^{-1}$), the dielectric anomaly was hardly observed. In general, almost no (or only a very small) anomaly was observed in the first cooling run ($T_H \rightarrow T_L$: $T_H = 285\text{--}310\text{ K}$, $T_L = 100\text{--}205\text{ K}$). However, in the subsequent heating run ($T_L \rightarrow T_H$), an increase in the dielectric constant began to appear above 270 K when the heating speed was sufficiently small. In general, the dielectric peak became extraordinarily large when the heating speed was very small, near 270–283 K ($< 2^\circ \text{h}^{-1}$). In Figure 3a, an example of the temperature dependences of the dielectric constants (ϵ_1) in the first cooling and heating runs and those in the second runs is presented. In this sample crystal, the growth of the dielectric anomaly was very smooth, and an extremely large enhancement of the dielectric constant was observed near 275 K, even in the first heating cycle in which the temperature was increased from 270 to 280 K over approximately 6 h. In general, a very large peak ($\epsilon_1 > 10^5$ at 1 kHz) appeared above 275 K in the second or third temperature cycle. The development of the peak was usually saturated after two to four cycles. In contrast, the large dielectric peak tended to disappear again when the crystal was heated to 320–330 K.

From this dielectric behavior, we conjectured that many small domains with extremely large polarizabilities were gradually grown in the crystal during the slow heating and cooling of the crystal in the range 230–285 K. However, these highly polarizable domains tend to disappear above 310 K, and the crystal seems to return to the initial low polarizability state. As shown in Figure 3, the maximum values of ϵ_1 reached an extremely large value of about 7×10^5 at 1 kHz, and ϵ_1 became larger than 10^4 over a very wide temperature range (220–320 K at 1 kHz).

The frequency dependence of the dielectric constant was also examined. As shown in Figure 3b, ϵ_1 showed a very strong frequency dependence. The capacitance (C) of the sample crystal was decreased by almost one order of magnitude when the frequency (ω) was increased tenfold, while the resistivity (R) of the crystal showed very small frequency dependence. Consequently, the loss tangent ($\tan \delta = \epsilon_2/\epsilon_1 \approx (\omega CR)^{-1}$) was approximately constant (ca. 3.5) in the temperature range in which the broad dielectric peak was observed (210–310 K; Figure 3b). The attempt to observe the dielectric hysteresis loop was performed near 260 K up to about 8 kV cm^{-1} . However, no clear hysteresis loop was observed under these conditions. This anomalous dielectric behavior of $[(\text{CH}_2)_3\text{NH}_2][\text{Cu}(\text{HCOO})_3]$, which has never been reported in the molecule-based dielectrics, remind us the behavior of so-called relaxor.

To obtain more detailed structural information, X-ray diffraction experiments were performed at 123–333 K. Smooth temperature dependence of the lattice constant was obtained above 288 K (Figure 4a). However, the data points were fairly scattered below 284 K. This result is mainly due to the appearance of additional X-ray diffraction spots indicating the structural change accompanying the change of crystal symmetry near 286 K; this temperature agrees well with the temperature of the broad maximum of the dielectric constant (Figure 3). X-ray diffraction patterns were examined at various temperatures (288 (initial temperature), 284, 278, 263, 233, 298, and 323 K (final temperature)). Although the crystal symmetry changed from orthorhombic to monoclinic near 286 K, the diffraction pattern at 284 K was almost identical to that observed at 288 K. However, below 278 K, extra X-ray diffraction spots were clearly observed (Figure 4b). It is easily imagined that monoclinic domains with slightly different orientations will develop in the crystal when the mirror symmetry of the orthorhombic lattice is lost by the freezing of the molecular deformation of the azetidinium cation. This behavior may be the main reason why the X-ray diffraction pattern changed below 278 K. The X-ray diffraction pattern taken at 298 K after cooling the crystal down to 233 K showed no extra diffraction spot. No significant difference could be observed between the initial X-ray diffraction pattern recorded at 288 K and the patterns recorded at 298 and 323 K after the low-temperature experiments. This result indicates that the crystal quality was almost unchanged by the cooling and heating processes. The crystal structure determined at 123, 180, 243, 260, 300, and 333 K indicated the increase of ring-puckering distortion of the azetidinium cation with a decrease in temperature (Figure 2c): the dihedral angle between the C1–N–C3 and the C1–

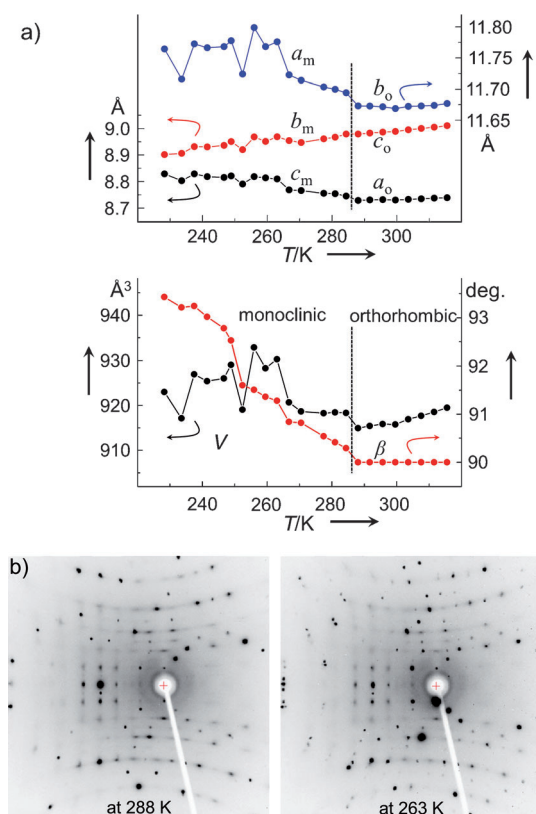


Figure 4. a) Temperature dependences of the lattice constants. The a , b , and c axes of the room-temperature orthorhombic lattice become the c , a , and b axes of the low-temperature monoclinic lattice, respectively. In this figure, a_o (a_m), b_o (b_m), and c_o (c_m) represent the lattice constants of the orthorhombic (monoclinic) lattice. b) X-ray diffraction patterns at 288 and 263 K.

C2–C3 planes is 180° above 286 K (orthorhombic phase), 158.6° at 260 K, 155.9° at 243 K, 154.4° at 180 K, and 153.7° at 123 K. The angle of out-of-plane bending deformation (the dihedral angle $\theta = 180^\circ$, Figure 2c) was about 26° at low temperature.

In summary, we have observed an extraordinarily large, broad peak for the dielectric constant for the metal formate perovskite $[(\text{CH}_2)_3\text{NH}_2][\text{Cu}(\text{HCOO})_3]$, which contains four-membered-ring ammonium cations. The dielectric constant became larger than 10^4 at 220–320 K and 1 kHz and reached 7×10^5 at 1 kHz near 280 K. The X-ray diffraction experiments revealed the change of the crystal symmetry from orthorhombic $Pmna$ to monoclinic $P2_1/c$ near 286 K. The azetidinium cation adopts a planar structure in the orthorhombic structure and a puckered structure in the low-temperature monoclinic structure. It is highly possible that the inherent conformational instability of the four-membered ring ammonium cation plays an essential role in inducing the change of the lattice symmetry of the metal–organic perovskite and the extraordinarily large dielectric anomaly. The present results will suggest a new route for the development of molecule-based systems with giant polarizabilities.

Experimental Section

Crystals of $[(\text{CH}_2)_3\text{NH}_2][\text{Cu}(\text{HCOO})_3]$ were prepared by the solution diffusion method according to the reported procedure.^[9] All the starting materials ($\text{Cu}(\text{NO}_3)_2 \cdot 3\text{H}_2\text{O}$, $(\text{CH}_2)_3\text{NH}$, HCOOH) are commercially available and were used without further purification. The X-ray diffraction experiments were carried out with a Rigaku Mercury CCD diffractometer with $\text{MoK}\alpha$ ($\lambda = 0.7107 \text{ \AA}$) at 123–333 K. The indexing of the diffraction spots at low temperatures ($< T_c$, ca. 286 K) was performed using the Twinsolve module of CrystalClear (Rigaku Corporation Inc.). The lattice constants of the room-temperature structure with an orthorhombic lattice and the space group $Pmna$ are $a = 8.721(1)$, $b = 11.653(2)$, $c = 8.977(1) \text{ \AA}$ at 300 K. The low-temperature structure has monoclinic symmetry and the space group $P2_1/c$, $a = 11.656(2)$, $b = 8.741(2)$, $c = 8.737(2) \text{ \AA}$, $\beta = 94.20(3)^\circ$ at 123 K. The a -glide symmetry of the orthorhombic lattice is retained in the monoclinic lattice as c -glide symmetry. The crystal structures were determined at 333 K (O), 300 K (O), 260 K (M), 243 K (M), 180 K (M), and 123 K (M), where O and M indicate orthorhombic and monoclinic structures, respectively. The R values were 3.58% at 333 K, 3.40% at 300 K, 7.33% at 260 K, 4.27% at 243 K, 4.49% at 180 K, and 2.92% at 123 K. The obtained low-temperature structure might be the “average structure” of various monoclinic domains developed below T_c . The low-temperature structure refinements were also performed by assuming the non-centrosymmetric space groups Pc and $P2_1$, but no improvement was achieved. CCDC 833127 (123K), 833310 (300K), 833311 (180K), 833312 (243K) and 833313 (333K) contain the supplementary crystallographic data for this paper. These data can be obtained free of charge from The Cambridge Crystallographic Data Centre via www.ccdc.cam.ac.uk/data_request/cif.

For the dielectric measurements, the crystals of $[(\text{CH}_2)_3\text{NH}_2][\text{Cu}(\text{HCOO})_3]$ were cut into rectangular parallelepipeds. The typical size of the crystal was $0.5 \times 0.8 \times 0.8 \text{ mm}^3$. Conducting gold paste was applied to the crystal surface for use as an electrode. The applied electric field was 1–0.2 V (or about 5–20 V cm^{-1}). The dielectric measurements were measured at 100 Hz–1 MHz. Since unexpectedly large capacitance (up to 10^{-7} F at 100 Hz) and fairly small resistance (down to about 5000 Ω) were observed near 280 K, we performed the dielectric measurements at 100 Hz, 1 kHz, 10 kHz, 100 kHz, and 1 MHz by attaching commercially available condensers (12 nF and 100 nF) and resistors (1 k Ω , 5 k Ω) to the sample holder instead of the crystal to check the reliability of the results of the measurements on the $[(\text{CH}_2)_3\text{NH}_2][\text{Cu}(\text{HCOO})_3]$ crystals. We confirmed that the correct capacitance and resistance were obtained, except at 1 MHz. The dielectric measurements were performed repeatedly for ten crystals. The broad dielectric anomaly near 280 K was observed for every crystal.

The lattice constants of $[(\text{CH}_2)_3\text{NH}_2][\text{Cu}(\text{HCOO})_3]$ crystal at various temperatures, and the temperature dependence of magnetic susceptibilities are presented in the Supporting Information.

Received: July 21, 2011

Published online: October 6, 2011

Keywords: dielectric constant · magnetic properties · organic–inorganic hybrid composites · perovskite phases · ring-puckering motion

- [1] Z. G. Lu, G. Calvarin, *Phys. Rev. B* **1995**, *51*, 2694–2702.
- [2] Y. M. Poplavko, *Ferroelectrics* **2004**, *298*, 253–259.
- [3] E. L. Venturini, R. K. Grubbs, G. A. Samara, Y. Bing, Z.-G. Ye, *Phys. Rev. B* **2006**, *74*, 064108.
- [4] a) H.-B. Cui, B. Zhou, L.-S. Long, Y. Okano, H. Kobayashi, A. Kobayashi, *Angew. Chem.* **2008**, *120*, 3424–3428; *Angew. Chem. Int. Ed.* **2008**, *47*, 3376–3380; b) B. Zhou, A. Kobayashi, H.-B.

- Cui, L.-S. Long, H. Fujimori, H. Kobayashi, *J. Am. Chem. Soc.* **2011**, *133*, 5736–5739; c) H.-X. Zhao, X.-J. Kong, H. Li, Y.-C. Jin, L.-S. Long, X. C. Zeng, R.-B. Huang, L.-S. Zheng, *Proc. Natl. Acad. Sci. USA* **2011**, *108*, 3481–3486.
- [5] a) S. Horiuchi, Y. Tokunaga, G. Giovannetti, S. Picozzi, H. Itoh, R. Shimano, R. Kumai, Y. Tokura, *Nature* **2010**, *463*, 789–792; b) T. Akutagawa, H. Koshinaka, D. Sato, S. Takeda, S. Noro, H. Takahashi, R. Kumai, Y. Tokura, T. Nakamura, *Nat. Mater.* **2009**, *8*, 342–347.
- [6] S. I. Chan, T. R. Borger, J. W. Russell, H. L. Strauss, W. D. Gwinn, *J. Chem. Phys.* **1966**, *44*, 1103–1111.
- [7] J. R. Durig, R. C. Lord, *J. Chem. Phys.* **1966**, *45*, 61–66.
- [8] T. Ueda, T. Shimanouchi, *J. Chem. Phys.* **1967**, *47*, 5018–5030.
- [9] Z. Wang, B. Zhang, T. Otsuka, K. Inoue, H. Kobayashi, M. Kurmoo, *Dalton Trans.* **2004**, 2209–2216.
- [10] X.-Y. Wang, L. Gan, S. W. Zhang, S. Gao, *Inorg. Chem.* **2004**, *43*, 4615–4625.
- [11] a) P. Jain, N. S. Dalal, B. H. Toby, H. W. Kroto, A. Cheetham, *J. Am. Chem. Soc.* **2008**, *130*, 10450–10451; b) P. Jain, V. Ramachandran, R. J. Clark, H. D. Zhou, B. H. Toby, N. S. Dalal, H. W. Kroto, A. K. Cheetham, *J. Am. Chem. Soc.* **2009**, *131*, 13625–13627.
- [12] G. C. Xu, X. M. Ma, L. Zhang, Z.-M. Wang, S. Gao, *J. Am. Chem. Soc.* **2010**, *132*, 9588–9590.
- [13] J. Laane, *Pure Appl. Chem.* **1987**, *59*, 1307–1326.
- [14] K. Hu, M. Kurmoo, Z. Wang, S. Gao, *Chem. Eur. J.* **2009**, *15*, 12050–12064.